Published in Computers inBiologyandMedicine54(2014)172–179

Recurring patterns of atrial fibrillation in surface ECG predict restoration of sinus rhythm by catheter ablation

Authors' names, academic degrees, and affiliations:
Luigi Yuri Di Marco[1,2], PhD; Daniel Raine[3], MBBS; John P. Bourke[3], MD; Philip Langley[1,4], PhD

[1]Institute of Cellular Medicine, Newcastle University, Newcastle upon Tyne, UK

[2] Centre for Computational Imaging and Simulation Technologies in Biomedicine (CISTIB), University of Sheffield, Sheffield, UK

[3]Department of Cardiology, Freeman Hospital, Newcastle upon Tyne Hospitals NHS Trust, Newcastle upon Tyne, UK

[4]School of Engineering, University of Hull, Hull, UK

Address for Correspondence:
Dr Luigi Yuri Di Marco
Centre for Computational Imaging and Simulation Technologies in Biomedicine (CISTIB)
Department of Mechanical Engineering
University of Sheffield
Sheffield
UK
Tel: +44 (0)114 2226074
luigiyuri.dimarco@gmail.com

Abstract

BACKGROUND: Non-invasive tools to help identify patients likely to benefit from catheter ablation (CA) of atrial fibrillation (AF) would facilitate personalised treatment planning.

AIM: To investigate atrial waveform organisation through recurrence plot indices (RPI) and their ability to predict CA outcome.

METHODS: One minute 12-lead ECG was recorded before CA from 62 patients with AF (32 paroxysmal AF; 45 men; age 57±10 years). Organisation of atrial waveforms from i) TQ intervals in V_1 and ii) QRST suppressed continuous AF waveforms (CAFW), were quantified using RPI: percentage recurrence (PR), percentage determinism (PD), entropy of recurrence (ER). Ability to predict acute (terminating vs. non-terminating AF), 3-month and 6-month postoperative outcome (AF vs AF free) were assessed.

RESULTS: RPI either by TQ or CAFW analysis did not change significantly with acute outcome. Patients arrhythmia-free at 6-month follow-up had higher organisation in TQ intervals by PD ($p<0.05$) and ER ($p<0.005$) and both were significant predictors of 6-month outcome (PD (AUC=0.67, $p<0.05$) and ER (AUC=0.72, $p<0.005$)). For paroxysmal AF cases, all RPI predicted 3-month (AUC(ER)=0.78, $p<0.05$; AUC(PD)=0.79, $p<0.05$; AUC(PR)=0.80, $p<0.01$) and 6-month (AUC(ER)=0.81, $p<0.005$; AUC(PD)=0.75, $p<0.05$; AUC(PR)=0.71, $p<0.05$) outcome. CAFW-derived RPIs did not predict acute or postoperative outcomes.

Higher values of any RPI from TQ (values greater than 25^{th} percentile of preoperative distribution) were associated with decreased risk of AF relapse at follow-up (hazard ratio ≤ 0.52, all $p<0.05$).

CONCLUSIONS: AF atrial waveform RPI could be used in selecting patients more likely to benefit from CA.

Keywords: Atrial fibrillation, TQ interval, recurrence quantification analysis, principal component analysis, electrocardiogram segmentation.

1. Introduction

There is considerable interest in developing tools capable of identifying patients likely to benefit from catheter ablation (CA) of AF. Termination of AF during CA is associated with longer-term maintenance of sinus rhythm (SR) [1-3]. Pre-ablation factors, such as AF cycle length (AFCL), left atrial diameter or volume, and duration of AF have been shown to predict the likelihood of termination [2,4]. Motivated by the clinical interest in non-invasive predictors of outcome from CA and electrical cardioversion the surface electrocardiogram (ECG) has also been studied. The f-wave, namely the atrial electrical signal (mainly observable in the TQ interval) has drawn considerable attention. Its amplitude and cycle length in preprocedural baseline recordings have been associated with acute [5-7] and intermediate [5,7] ablation outcomes. Techniques in the frequency or joint time-frequency domain, based on the spectral analysis of the estimated f-wave have also been applied to predict AF relapse following electrical cardioversion [8-10].

Recurrence quantification analysis, by Eckmann and colleagues [11] for the identification of dynamic patterns in time-series, has also been deployed in AF studies [12-15]. The method is based on a graphical representation, termed recurrence plot, of recurring patterns of sub-intervals of a given time-series. Indices can be calculated to quantify percentage, duration, and distribution of recurring patterns. The strength of this analysis is that it does not require modelling of the time-series, nor the removal of outliers [16].

At present, a quantitative non-invasive assessment of f-wave temporal predictability based on recurring patterns in individual ECG signals (auto-recurrence) is lacking, and might make prediction of acute and longer-term outcome following AF-ablation possible. In a previous study [17] we have successfully explored the ability of recurrence plot indices (RPIs) to predict acute and 3-month ablation outcome from preprocedural recordings of invasive intracardiac electrograms of the coronary sinus and right atrial appendage.

The aim of this study was to investigate the ability of RPIs from surface ECG recordings to predict acute and postoperative (3-month and 6-month) ablation outcome.

2. Methods

2.1 Study Population and Data Recording

62 consecutive patients with AF (32 paroxysmal AF, 30 persistent AF; 45 men; age 57±10 years) undergoing catheter ablation for standard clinical indications at this hospital were enrolled in the study. The characteristics of the patient cohort are summarised in Table 1; the sample partition with respect to AF classification (paroxysmal or persistent) and CA outcome are shown in Table 2.

Prior to any ablation, 12-lead ECG recordings of 1-minute duration were obtained (Labsystem Pro™ recording system (Bard EP, C. R. Bard, Inc.). The signal was digitised at a sample rate of 1000 samples/s and stored for offline processing.

2.2 Electrophysiology Study

The study was conducted in compliance with the ethical principles of the Declaration of Helsinki. Patients gave informed consent. Class I and III antiarrhythmic drugs were discontinued five half-lives prior to ablation.

Ablation comprised the following stages.

1. *PVI*

All patients underwent PVI. Pulmonary veins were isolated electrically using one of three ablation technologies: (I) PVAC® multi-electrode circumferential ablation catheter (Medtronic Ablation Frontiers); (II) Arctic Front® cryo-balloon (Medtronic Cryocath); and (III) wide-area circumferential ablation using ThermoCool® SmartTouch™ catheter and CARTO®3 electroanatomical mapping and navigation system (Biosense Webster). Electrical isolation was inferred by the absence of local electrograms distal to the sites of ablation or independent pulmonary vein activity and, in those patients in sinus rhythm, by demonstrating entrance and exit block between the pulmonary veins and left atrium using pacing manoeuvres.

2. *LA substrate ablation*

Patients who did not revert to sinus rhythm during pulmonary vein isolation received further left atrial ablation as follows:

a) CFAE ablation

A detailed analysis of the left atrium and inter-atrial septum was performed to identify CFAEs (focal sites exhibiting constant electrical activity, or multi-component electrograms with cycle length <120ms averaged over a 10-second period), which were then ablated. This process was completed when no residual CFAE sites could be identified in the body of the left atrium or inter-atrial septum or when sinus rhythm was restored by ablation.

b) *Linear ablation*

A combination of 'roof line' (connecting right and left upper pulmonary vein ostia), "mitral line" (connecting left lower pulmonary vein ostium to mitral valve annulus) and "inferior line" (connecting right lower pulmonary vein to coronary sinus) was constructed depending on the degree of signal complexity at the various sites. Linear ablation was performed with the endpoint being the absence of electrograms and presence of double potentials along the length of each line. No differential pacing manoeuvres were performed.

Of 32 paroxysmal AF patients, 24 had PVI only; 7 had PVI and linear ablation; and one had PVI, CFAE and linear. Of 30 persistent AF patients, 5 had PVI only; 6 PVI and linear; 11 had PVI and CFAE; and 8 had PVI, CFAE and linear ablation. The mean procedure and fluoroscopy times for the 62 patients were 191 ± 36 and 33 ± 16 minutes, respectively.

All patients in AF at the end of the ablation procedure were labelled as "non-terminated" AF (NT-AF), the others as "terminated" AF (T-AF) and this defined the acute outcome. Patients with non-terminated AF subsequently received electrical cardioversion. Clinical outcome was further assessed three and six months after ablation (or electrical cardioversion if performed) by symptom review, 12-lead ECG and 72-hour Holter recordings. AF recurrence was defined as the presence of arrhythmia symptoms with documented AF on a 12-lead ECG and/or AF episodes lasting at least 30 seconds on Holter monitoring. Early relapse within the first 3 months of CA is known to occur in some patients who subsequently

maintain SR in the longer term. In line with other studies we observed a 3-month blanking period, where recurrence in this period is discarded in terms of the longer follow-up period (6 months).

At 3-month and 6-month follow-up, AF was detected in 19 and 21 patients, respectively (Table 2).

2.3 Signal Processing

As the body surface AF waveform is free of obscuring ventricular activity only during the TQ interval of the cardiac cycle, we conducted our analysis firstly on AF waveforms extracted from TQ intervals, and secondly on the continuous AF waveform (CAFW) derived by suppression of the QRS-T by principal component analysis (PCA).

The ECG signals were preliminarily filtered to remove baseline wander due to respiration (4^{th} order Butterworth high-pass filter with 3dB cut-off frequency of 0.5 Hz) and mains (notch filter at 50 Hz).

2.3.1 Automated identification of QRS-T intervals

The ECG lead II was segmented using an automated algorithm inspired by Di Marco and Chiari [18], based on discrete *wavelet* transforms, to identify the QRS-T intervals. Briefly, the algorithm consists of two stages. In the first, beat detection is performed to identify the QRS complex of each ventricular contraction, then the fiducial points (i.e. the sample indices in the digital ECG data) indicating the onset of the QRS and the end of the T wave are determined.

The collection of sample indices of all QRS-T intervals (W_{QRST}) was retained for recurrence analysis of TQ intervals of lead V_1. An example of the algorithm's detected QRS-T window for consecutive ventricular contractions is illustrated in Figure 1. The horizontal lines in the left panels indicate data samples pertaining to a QRS-T interval (calculated from lead II, also displayed).

2.3.2 Continuous AF waveform by Principal Component Analysis

PCA is a source separation technique capable of estimating the continuous AF waveform (CAFW) from the surface ECG [19-20] with performance comparable to alternative extraction algorithms such as QRST template subtraction [21]. PCA was performed on a set of three quasi-orthogonal leads (I, aV_F,

V_1). In agreement with Raine and colleagues [20], it was visually verified that the 1st principal component (PC1) had a prominent ventricular component, which was less dominant in other components. In particular it was visually observed that atrial activity was dominant and ventricular contaminants were minimised in PC_3.

2.3.3 Recurrence quantification analysis

The presence of repeating (recurring) patterns of the atrial waveform was assessed by auto-recurrence quantification analysis. The method is based on a graphical representation of the similarity of subintervals of fixed length *m*, known as *embedding dimension*. On a square matrix, each point at coordinates *(i,j)* represents the similarity between two subintervals x_i and x_j both of length *m*. If the two subintervals are similar (i.e. their modulus distance is within a fixed tolerance ε) the point (i, j) on the matrix will be set to 1, otherwise it will be set to 0. Mathematically:

$$R_{i,j} = \Theta(\varepsilon - \|\mathbf{x}_i - \mathbf{x}_j\|) \quad i, j = 1,2,...,M \tag{1}$$

where $R_{i,j}$ is the *(i,j)*th element of the recurrence matrix, $\Theta(\cdot)$ is the Heaviside function, $M = N-(m-1)$, N is the number of points in the time-series. The norm $\|\cdot\|$ represents the Euclidean distance operator, $\mathbf{x}_i = (x_i \ \ldots \ x_{i+m-1})^T$, and $(\cdot)^T$ is the transposed operator. This formulation assumes a delay constant $\tau = 1$ (1 sample). Here, *x* is the ECG atrial waveform. The recurrence matrix can be represented graphically by the recurrence plot as illustrated in Figure 1. In the recurrence plot pixels corresponding to elements of *R* of value 1 are coloured black while those of value 0 are coloured white.

Equation 1 was used for analysis of the CAFW. However, for analysis of TQ intervals, elements of *R* corresponding to QRS-T intervals were assigned to infinite, namely arbitrarily high distance from any other point in the time series. Mathematically this corresponds to a modification in eq. (1), as follows:

$$R_{i,j} = \begin{cases} \infty & i \in W_{QRST} \quad or \quad j \in W_{QRST} \\ \Theta(\varepsilon - \|\mathbf{x}_i - \mathbf{x}_j\|) & otherwise \end{cases} \tag{2}$$

where W_{QRST} is the collection of all QRS-T intervals in the entire recording. As a corollary of eq. (2), points in QRS-T intervals were treated as non-recurring. Thus, the analysis of recurrence was limited to

TQ intervals of the ECG in lead V_1. The fraction of data containing TQ intervals in our dataset was 47.7 % ± 8.6% (mean ± std, across 62 records).

Recurrence plot indices

Percentage recurrence (PR, percentage of recurring subintervals $\boldsymbol{x}_i$), percentage determinism (PD, percentage of recurring $\boldsymbol{x}_i$ forming prolonged ('deterministic') recurrence lasting at least L_{MIN} (=15) consecutive $\boldsymbol{x}_i$), and entropy of recurrence (ER, entropy of recurring patterns lasting at least L_{MIN} consecutive $\boldsymbol{x}_i$) indices were calculated from the recurrence matrix [12,14]. The choice of the above indices was based on their ability to describe the recurring dynamics of a time series [22].

Mathematically:

$$
\begin{aligned}
PR &= \frac{1}{N^2}\sum_{i,j=1}^{N} R_{i,j} \cdot 100 \\
PD &= \frac{\sum_{l=L_{MIN}}^{N} l\, H_l}{\sum_{i,j=1}^{N} R_{i,j}} \cdot 100 \\
ER &= -\sum_{l=L_{MIN}}^{N} p_l \log_2 p_l \\
p_l &= \frac{H_l}{\sum_{l=L_{MIN}}^{N} H_l}
\end{aligned}
\qquad (3)
$$

where H_l is the proportion of diagonals of length l in the recurrence matrix R, p_l is the probability that a diagonal has length l. The index l ranges from L_{MIN} to the length N of the time series being analysed.

The maximum length of recurrence (L_{MAX}) was also calculated:

$$L_{MAX} = \max_{k\in\{1,\ldots,N_D\}} \{l_k\} \qquad (4)$$

where N_D is the number of diagonal lines in the recurrence plot, and l_k is the length (number of points) of the kth diagonal line.

Higher values of recurrence indices indicate greater determinism and more organised atrial waveform.

To reduce the computational burden, without loss of information, the ECG signal was down-sampled at 100 samples/s (using anti-alias low-pass filtering) prior to computation of RPIs.

Selection of recurrence plot parameters

A standard criterion to select the recurrence plot parameters (time delay (τ), similarity tolerance (ε), and minimum length (L_{MIN})) is lacking. It is generally accepted that the choice depends on the data [12-14,16,22]. In this study, the time delay was set to 1, as suggested in [16]. A suitable value for *m* (=11) was determined using the *false nearest neighbour* criterion [23] with tolerance threshold of 10%. At a sample rate of 100 Hz, the chosen value for *m* corresponds to 110 ms. For the threshold ε, a similar method to the one proposed by Censi and colleagues [12] was used. The value for ε was empirically set to a fraction (K_ε = 25%) of the 3rd quartile of the ($\boldsymbol{x}_i$, $\boldsymbol{x}_j$) distance distribution. The values of K_ε and L_{MIN} were chosen based on a sensitivity analysis illustrated in Figures 2–3. Figure 2 shows the PR distribution over the study population (N=62) as a function of K_ε. Larger distribution (larger inter-quartile range, vertical bars in Figure 2) of PR is visible in the linear region of the sigmoid compared to the saturation regions, consistently with previous observations [24]. Conversely, the saturation regions are characterised by either very small values of K_ε (too strict similarity criteria, hence very few $\boldsymbol{x}_i$ subintervals are detected as similar, leading to very low PR and PR variability) or very high values (too large similarity criteria, hence almost all $\boldsymbol{x}_i$ are detected as similar, leading to very high PR and low PR variability). Therefore, the best choice for K_ε appears to be in the linear region of the sigmoid (i.e. between 15% and 30%). Note that by construction, PR does not depend on L_{MIN}.

Figure 3 shows PD and ER distributions as function of K_ε and L_{MIN}. Both PD and ER increased monotonically with K_ε independently of L_{MIN} delineating a saturating curve, similar to the sigmoid pattern described above. For increasing values of L_{MIN}, PD increased with stable distribution over the study population, whereas ER was very marginally affected. We therefore adopted an intermediate value for L_{MIN} (150 ms, central trace in Figure 3).

Owing to space limitations, the results of our study are reported for the chosen values of K_ε (25%) and L_{MIN} (150 ms); however, the robustness of the method (i.e. consistency of the results in magnitude and significance) was verified over a set values for K_ε in the linear region of the PR sigmoid (i.e. K_ε = 15%, 20%, 25%, 30%) and for L_{MIN} = 100 ms, 150 ms, 200 ms.

2.3.4 f-wave amplitude in TQ intervals

The f-wave amplitude was calculated from lead V_1 as the peak-to-nadir voltage difference in the TQ intervals (ΔT_{TQ}) satisfying the condition:

$$\Delta T_{TQ} \geq \frac{1}{F_{MIN}} \tag{5}$$

where F_{MIN} (= 3.5 Hz) is the lowest frequency in the AF spectrum of interest [19]. By construction, TQ intervals satisfying the above condition contained at least one full AF cycle.

It was verified that the above condition was met by at least 8 TQ intervals in each recording. The median TQ amplitude obtained from such intervals in each recording was retained for statistical analysis.

To prevent bias due to residual baseline wander, the linear trend was subtracted from the TQ interval prior to calculation of f-wave amplitude.

Statistical Analysis

The ability of individual RPIs to predict acute and postoperative outcome was assessed by calculating the area under the curve (AUC) of the *receiver operating characteristic* (ROC). Cox proportional hazards regression models were used to estimate the hazard ratios (HR) of postoperative AF relapse, with time to event calculated as follow-up period (3 and 6 month). Group comparisons were performed using Mann-Whitney test (2-tail), with significance level of 0.05. The statistical analysis was done using SPSS statistical software (IBM Corp., Armonk, NY) and MATLAB Statistical Toolbox (The Mathworks, Inc, Natick, MA).

3. Results

3.1 Characterisation of acute and postoperative ablation outcome

3.1.1 Analysis of TQ intervals

Recurrence plot indices

The recurrence indices from TQ intervals did not show significant difference between the acute outcome groups (terminated vs. non-terminated AF) (Table 3). ER was significantly different between outcome groups (arrhythmia-free vs. AF relapse) at 3-month follow-up ($p<0.05$) and had increased statistical significance at 6-month follow-up ($p<0.005$). PD was also significantly different between the groups at 6-month follow-up ($p<0.05$). Furthermore, patients who would be arrhythmia-free at follow-up had higher values for all recurrence indices, indicating higher degree of determinism of the f-wave in TQ intervals.

The maximum length of recurrence (L_{MAX}) was not significantly different either with respect to acute or postoperative outcome groups, regardless of the original signal (TQ interval vs. CAFW). For the sake of space, the results referring to L_{MAX} are not shown in the tables.

To assess the consistency of the results with respect to the recurrence plot parameters (K_ε and L_{MIN}), these parameters were changed over the rectangular grid defined by: K_ε = 15%, 20%, 25%, 30%; and L_{MIN} = 100 ms, 150 ms, and 200 ms. For each point in the grid the analysis was repeated, and it was observed that the sign and significance ($p<0.05$) of group differences was preserved.

AF subgroup analysis

Since the majority of patients terminating AF during CA were paroxysmal cases (Table 2), a subgroup analysis for acute outcome was undertaken considering only patients with paroxysmal AF. Group differences (T-AF vs. NT-AF) were no longer significant for all indices.

Postoperative outcome was assessed separately for the paroxysmal and persistent AF groups (Table 4). For the paroxysmal AF group significant differences in the postoperative outcome (both at 3-month and 6-month) were observed in all RPIs. Again, patients who would be arrhythmia-free at follow-up had higher values for all recurrence indices. A similar difference in median values was also observed for persistent AF patients, however none of the indices reached statistical significance (Table 4).

f-wave amplitude

The f-wave amplitude was lower in the terminated compared to the non-terminated AF group, and in the arrhythmia-free at follow-up (3 and 6 month) compared to the AF relapse groups. However, the difference was not significant for the acute outcome, and was nearly significant for the 3-month ($p=0.05$)

and 6-month (p=0.07) outcome (Table 3). This trend was also observed in the AF subgroup analysis of postoperative outcome, considering paroxysmal and persistent AF separately (Table 4). Since amplitude was not significantly different for either acute or postoperative outcome, it was not considered for further analysis.

3.1.2 Analysis of CAFW

For CAFW (Table 5) median recurrence indices were greater in terminating and NSR groups in accord with the TQ analysis results, however the difference between groups did not reach a significant level for any of the indices.

3.2 Prediction of postoperative outcome

3.2.1 Analysis of TQ intervals

Recurrence plot indices

PD and ER from TQ intervals were significant individual predictors of 6-month outcome (Table 6). Three-month outcome was also predicted by ER ($p<0.05$), however, longer term outcome was predicted with stronger significance.

AF subgroup analysis

For the paroxysmal AF group, all RPIs were significant individual predictors of postoperative outcome, both at 3- and 6-month follow-up (Table 6). The overlapping confidence intervals, however, suggest similar predictive ability of the RPIs. On the other hand, in the persistent AF group, none of the indices could predict the clinical outcome.

Risk of AF relapse

The association between RPIs from TQ intervals and the risk of AF relapse was also assessed. For each RPI, arbitrary thresholds were set at 25^{th}, 50^{th} and 75^{th} percentiles of the index distribution across the entire population (N=62). For each threshold value, the association between the index (categorised as above/below the threshold) and postoperative outcome was quantified (Table 7). For first (25%) and second (50%) quartile cut-off, patients with any RPI higher than the cut-off value had significantly reduced risk of AF relapse. ER showed the strongest association, with 65% reduction of AF relapse risk (HR = 0.35, $p<0.001$) in patients with ER greater than the 25^{th} percentile.

3.2.2 Analysis of CAFW

CAFW indices were unable to predict postoperative outcome, regardless of the length of follow-up (data not shown).

4. Discussion

4.1 Characterisation of acute and postoperative ablation outcome

RPIs from TQ intervals were significantly higher in patients who remained arrhythmia-free at 6-month follow-up (Table 3), and even more significantly for paroxysmal AF patients (Table 4). Higher RPIs values indicated that preprocedural ECG recordings had greater repetitiveness and increased determinism of atrial activity in these patients compared to those with AF-relapse. This suggests that RPIs are useful in predicting ablation success in the intermediate (6-month) term, in particular for the paroxysmal AF patients (Table 6), and agrees with the general observation that CA is more likely to be successful in patients with more organised AF.

The results from the present study are broadly consistent with those from our previous study [17] on intracardiac recordings in the same patients. However, in that study we found that RPIs of invasive recordings were also able to predict acute (T-AF vs. NT-AF) outcome while in the present study indices from non-invasive recordings could not. As the number of T-AF patients is small (N=12) compared to

the overall sample (N=62), the difference between the two studies could be explained by the presence of noisy excerpts either in the intracardiac signals of the previous study or in the surface electrical signals of the present study. However, there is also the possibility that some characteristics of the atrial wavefront dynamics are lost at the surface, as neither TQ nor CAFW analysis were able to identify them, at least at the body sites investigated.

Our results suggest the presence of *latent* f-wave dynamics that manifest at a later stage after CA. This hypothesis is supported by the increasing predictivity (increasing number of significant predictors and increasing significance of AUC) observed with longer term follow-up (Table 6).

TQ amplitude was not sensitive to the acute outcome, whereas it was weakly sensitive to the 3-month ($p=0.05$) and the 6-month outcomes ($p=0.07$, Table 3), showing lower values for the patients who would be arrhythmia-free at follow-up. This result is in contrast with that of Nault and colleagues [7] who found higher f-wave amplitude at baseline to predict AF termination during ablation, and to be associated with a reduced rate of AF relapse. However, as noted in [6], methods based on manual estimation of the f-wave amplitude are inherently associated with inter-observer variability, which could explain the contrasting results. Many patients exhibit significant temporal variability of body surface AF amplitude, therefore its measurement is subject to sample variation. To avoid this bias we adopted an automated approach using the median of TQ intervals whose duration was sufficient to contain at least one full AF cycle at the lowest fibrillatory rate (Eq. 5).

When stratified by AF classification, the analysis of persistent AF patients did not show any significant difference in RPIs with respect to postoperative outcome (Table 4). This was also observed for acute outcome (data not shown).

4.2 Risk of AF relapse

For all RPIs obtained from TQ intervals, higher values at baseline (preprocedural) were associated with reduced risk of AF relapse (Table 7). It is worth noting that this analysis was based on *a priori* knowledge of the data. In other words, the threshold for categorising recurrence indices (‘low’, ‘high‘) was not calculated from ROC analysis (optimal threshold), it was calculated from the *prior* distribution

(unconditional upon CA outcome) of the preprocedural data. This approach is less sensitive to the bias generated by ROC-optimal thresholding.

Furthermore, the significant and consistent results, both in orientation and magnitude of risk, for different thresholds (1st and 2nd quartile), suggest this approach is robust with respect to outliers in the data distribution. This offers a potential use in the clinical setting, in which a short (1-minute) preprocedural ECG recording could contribute to identifying patients at higher risk of AF relapse.

4.3 Comparison of TQ and CAFW indices predictivity

Although median values for RPIs from CAFW were higher for successful compared to unsuccessful outcome (Table 5) in accordance with TQ analysis (Tables 3 and 4), the difference between groups in CAFW indices did not reach significant levels in either outcome. This was also the case when the paroxysmal and persistent AF groups were analysed separately (data not shown).

This could be explained either by the presence of sporadic residual ventricular contamination in the f-waveform estimated by PCA [20] and other f-wave estimation techniques, or by the different length in the TQ and CAFW signals (in the former only TQ intervals are analysed, in the latter the whole recording). To test these hypotheses, the CAFW analysis was repeated, confined to intervals of PC_3 which corresponded to the TQ intervals (data not shown). The results remained not significant, suggesting that CAFW-derived RPIs are not predictive of either acute or postoperative outcomes.

Our results are in contrast with another study on surface ECG [25], in which a weighted PCA-based method predicted postoperative CA outcome in a sample of 20 persistent-AF patients over a variable (on a patient basis) follow-up period between 4 and 19 months. Although the discordance could at least in part be explained by the different sample size and variable follow-up period in [25], the significant predictivity obtained in the above study suggests that more advanced multi-lead approaches could improve the predictivity of CA clinical outcome.

However, these results support the validity of recurrence plot analysis applied to TQ intervals only, avoiding the need for the laborious QRS-T cancellation.

4.4 Study limitations

The present study may be limited because the number of patients studied is relatively small (although comparable to other reported studies) and recruited from a single centre.

An automated ECG segmentation approach may be less accurate than a human expert, especially in the annotation of the T wave end in noisy signals. However, an automated approach is not biased by inter-observer variability.

The differences in the ablation approach to achieve the predefined endpoint could have played a role in the ablation outcome. However, the protocol described in this study is typical of clinical practice with persistent AF patients commonly having left atrial substrate ablation in addition to pulmonary vein isolation at a first procedure.

The successful acute outcome rate was 19.4%. Other studies have achieved higher AF termination rates using different ablation protocols with restoration of SR as the procedural endpoint [1,3]. Therefore further validation of our algorithms on datasets with a higher incidence of AF termination is required, as this might correlate with lower rates of AF relapse in the six month period following ablation.

5. Conclusions

Quantitative evidence of recurring patterns of atrial wavefront (f-wave) in TQ intervals of ECG lead V_1 was shown in preprocedural 1-minute recordings. PD and ER were significant individual predictors of 6-month CA outcome.

Higher values of either PR, PD, or ER (based on *a priori* thresholds calculated from the preoperative distribution of the given index) were associated with decreased risk of AF relapse at 3- and 6- month follow-up. TQ-RPIs, in particular ER, could be used to identify patients more likely to benefit from CA.

Acknowledgement

This work was funded partly by the National Institute for Health Research Newcastle Biomedical Research Centre based at Newcastle Hospitals Foundation Trust and Newcastle University (PL) and by a British Heart Foundation Clinical Research Fellowship (DR). The authors declare there are no conflicts of interest related to this work.

References

1. C.S. Elayi, L. Di Biase, C. Barrett, C.K. Ching, M. al Aly, M. Lucciola, R. Bai, R. Horton, T.S. Fahmy, A. Verma, Y. Khaykin, J. Shah, G. Morales, R. Hongo, S. Hao, S. Beheiry, M. Arruda, R.A. Schweikert, J. Cummings, J.D. Burkhardt, P. Wang, A. Al-Ahmad, B. Cauchemez, F. Gaita, A. Natale. Atrial fibrillation termination as a procedural endpoint during ablation in long-standing persistent atrial fibrillation. Heart Rhythm. 7 (2010) 1216–23.

2. A. Forclaz, S.M. Narayan, D. Scherr, N. Linton, A.S. Jadidi, I. Nault, L. Rivard, S. Miyazaki, L. Uldry, M. Wright, A.J. Shah, X. Liu, O. Xhaet, N. Derval, S. Knecht, F. Sacher, P. Jaïs, M. Hocini, M. Haïssaguerre. Early temporal and spatial regularization of persistent atrial fibrillation predicts termination and arrhythmia-free outcome. Heart Rhythm. 8 (2011) 1374–82.

3. E.K. Heist, F. Chalhoub, C. Conor Barrett, S. Danik, J.N. Ruskin, M. Mansour. Predictors of atrial fibrillation termination and clinical success of catheter ablation of persistent atrial fibrillation. Am J Cardiol 110 (2012) 545–551.

4. I. Drewitz, S. Willems, T.V. Salukhe, D. Steven, B.A. Hoffmann, H. Servatius, K. Bock, M.A. Aydin, K. Wegscheider, T. Meinertz, T. Rostock. Atrial fibrillation cycle length is a sole independent predictor of a substrate for consecutive arrhythmias in patients with persistent atrial fibrillation. Circ Arrhythm Electrophysiol. 3 (2010) 351–60.

5. S. Matsuo, N. Lellouche, M. Wright, M. Bevilacqua, S. Knecht, I Nault, K.T. Lim, L. Arantes, M.D. O'Neill, P.G. Platonov, J. Carlson, F. Sacher, M. Hocini, P. Jaïs, M. Haïssaguerre. Clinical predictors of termination and clinical outcome of catheter ablation for persistent atrial fibrillation. J Am Coll Cardiol. 54 (2009) 788–95.

6. M. Meo, V. Zarzoso, O. Meste, D. Latcu, N. Saoudi. Spatial variability of the 12-lead surface ECG as a tool for noninvasive prediction of catheter ablation outcome in persistent atrial fibrillation. IEEE Trans Biomed Eng. 60 (2013) 20–7.

7. I. Nault, N. Lellouche, S. Matsuo, S. Knecht, M. Wright, K.T. Lim, F. Sacher, P. Platonov, A. Deplagne, P. Bordachar, N. Derval, M.D. O'Neill, G.J. Klein, M. Hocini, P. Jaïs, J. Clémenty, M. Haïssaguerre. Clinical value of fibrillatory wave amplitude on surface ECG in patients with persistent atrial fibrillation. J Interv Card Electrophysiol. 26 (2009) 11–9.

8. R. Alcaraz, J.J. Rieta. Time and frequency recurrence analysis of persistent atrial fibrillation after electrical cardioversion. Physiol Meas. 30 (2009) 479–89.

9. R. Alcaraz, J.J. Rieta. Application of Wavelet Entropy to predict atrial fibrillation progression from the surface ECG. Comput Math Methods Med. (2012) 2012:245213.

10. A. Bollmann, D. Husser, R. Steinert, M. Stridh, L. Soernmo, S.B. Olsson, D. Polywka, J. Molling, C. Geller, H.U. Klein. Echocardiographic and electrocardiographic predictors for atrial fibrillation recurrence following cardioversion. J Cardiovasc Electrophysiol. 14 (2003) S162–5.

11. J.P. Eckmann, S.O. Kamphorst, D. Ruelle. Recurrence plots of dynamical systems. Europhys Lett. 4 (1987) 973–7.

12. F. Censi, V. Barbaro, P. Bartolini, G. Calcagnini, A. Michelucci, G.F. Gensini, S. Cerutti. Recurrent patterns of atrial depolarization during atrial fibrillation assessed by recurrence plot quantification. Ann Biomed Eng. 28 (2000) 61–70.

13. M. Mohebbi, H. Ghassemian. Prediction of paroxysmal atrial fibrillation using recurrence plot-based features of the RR-interval signal. Physiol Meas. 32 (2011) 1147–62.

14. M. Mohebbi, H. Ghassemian, B.M. Asl. Structures of the recurrence plot of heart rate variability signal as a tool for predicting the onset of paroxysmal atrial fibrillation. J Med Signals Sens. 1 (2011) 113–21.

15. R. Sun, Y. Wang. Predicting termination of atrial fibrillation based on the structure and quantification of the recurrence plot. Med Eng Phys. 30 (2008) 1105–11.

16. C.L. Webber Jr. Recurrence quantification of fractal structures. Front Physiol. 3 (2012) 382.

17. L.Y. Di Marco, D. Raine, J.P. Bourke, P. Langley. Characteristics of atrial fibrillation cycle length predict restoration of sinus rhythm by catheter ablation. Heart Rhythm. 10 (2013) 1303–10.

18. L.Y. Di Marco, L. Chiari. A wavelet-based ECG delineation algorithm for 32-bit integer online processing. Biomed Eng Online. 10 (2011) 23.

19. A. Bollmann, D. Husser, L. Mainardi, F. Lombardi, P. Langley, A. Murray, J.J. Rieta, J. Millet, S.B. Olsson, M. Stridh, L. Sörnmo. Analysis of surface electrocardiograms in atrial fibrillation: techniques, research, and clinical applications. Europace. 8 (2006) 911–26.

20. D. Raine, P. Langley, A. Murray, A. Dunuwille, J.P. Bourke. Surface atrial frequency analysis in patients with atrial fibrillation: a tool for evaluating the effects of intervention. J Cardiovasc Electrophysiol. 15 (2004) 1021–6.

21. P. Langley, J.J. Rieta, M. Stridh, J Millet-Roig, L. Sörnmo, A. Murray. Comparison of atrial signal extraction algorithms in 12-lead ECGs with atrial fibrillation. IEEE T Bio-Med Eng, 53 (2006) 343-346.

22. C.L. Webber Jr, J.P. Zbilut. Dynamical assessment of physiological systems and states using recurrence plot strategies. J Appl Physiol. 76 (1994) 965–73.

23. M.B. Kennel, R. Brown, H.D. Abarbanel. Determining embedding dimension for phase-space reconstruction using a geometrical construction. Phys Rev A. 45 (1992) 3403–3411.

24. C.L. Webber, Jr., J.P. Zbilut. Recurrence quantification analysis of nonlinear dynamical systems. In Tutorials In Contemporary Nonlinear Methods for the Behavioral Sciences, Chap.2, eds M.A.Riley and G. Van Orden (Arlington,VA: National Science Foundation). (2005) 26–94.

25. M. Meo, V. Zarzoso, O. Meste, D.G. Latcu, N. Saoudi. Catheter ablation outcome prediction in persistent atrial fibrillation using weighted principal component analysis. Biomedical Signal Processing and Control. 8 (2013) 958–968.

Tables

Table 1. Study Population

	All	Acute outcome Sinus Rhythm Restored	
		Yes (T-AF)	No (NT-AF)
Patients	62	12 (19%)	50 (81%)
Women	17	4 (24%)	13 (76%)
Age [years] (mean±SD)	57±10	61±9	56±10
AF history duration [years] (mean±SD)	5±4	4±3	5±5
LV ejection fraction [%]	52±6	54±2	52±7
LA volume [ml]	59±18	59±20	58±18
Betablockers	51	9 (18%)	42 (82%)
Calcium antagonists (Diltiazem, Verapamil)	3	1 (33%)	2 (67%)
Antiarrhythmic (withdrawn 5 half lives pre-CA)			
Amiodarone*	2	0 (0%)	2 (100%)
Dronedarone	1	0 (0%)	1 (100%)
Flecainide	15	5 (33%)	10 (67%)
Propafenone	2	1 (50%)	1 (50%)
Sotalol	2	0 (0%)	2 (100%)
Anticoagulant			
Dabigatran	4	1 (25%)	3 (75%)
Warfarin	61	11 (18%)	50 (82%)
Further Ablation after PVI			
CFAE only	11	4 (36%)	7 (64%)
Linear only	13	1 (8%)	12 (92%)
CFAE + Linear	9	0 (0%)	9 (100%)

T-AF indicates “terminated” atrial fibrillation (AF); NT-AF, “non terminated” AF; LV, left ventricular; LA, left atrial; PVI, pulmonary vein isolation; CFAE, complex fractionated electrogram.

* Not withdrawn pre-CA

Table 2. Study population: partition of sample size

AF Substrate	Acute outcome		Postoperative outcome (3-month)		Postoperative outcome (6-month)		All
	T-AF	NT-AF	NSR	AF	NSR	AF	
Paroxysmal	11	21	23	9	20	12	32
Persistent	1	29	20	10	21	9	30
All	12	50	43	19	41	21	62

T-AF indicates “terminated” atrial fibrillation (AF); NT-AF, “non terminated” AF; NSR, normal sinus rhythm (at follow-up)

Table 3. Characterisation of outcome from TQ analysis. Values are Median(IQR)

Outcome	Percentage Recurrence [%]		p value	Percentage Determinism [%]		p value	Entropy of Recurrence [dimensionless]		p value	f-wave Ampl [μV]		p value
Acute	T-AF	NT-AF		T-AF	NT-AF		T-AF	NT-AF		T-AF	NT-AF	
	37.92(22.38)	43.36(37.82)	N.S.	35.76(12.89)	48.59(35.48)	N.S.	4.04(0.47)	4.26(0.83)	N.S.	133(77)	142(57)	N.S.
Postoperative (3 month)	NSR	AF		NSR	AF		NSR	AF		NSR	AF	
	46.37(25.56)	32.30(39.33)	N.S.	49.15(28.68)	35.11(33.93)	N.S.	4.32(0.62)	3.81(0.70)	<0.05	136(63)	157(108)	p=0.05
Postoperative (6 month)	NSR	AF		NSR	AF		NSR	AF		NSR	AF	
	46.37(26.80)	33.64(39.41)	N.S.	50.03(30.06)	35.11(25.86)	<0.05	4.36(0.66)	3.89(0.60)	<0.005	136(68)	151(59)	p=0.07

T-AF, terminated atrial fibrillation (AF); NT-AF, not terminated AF; NSR, normal sinus rhythm. $N_{T\text{-}AF}$=12, $N_{NT\text{-}AF}$ = 50. At 3-month (6-month) follow-up: N_{NSR}=43, N_{AF} = 19 (N_{NSR}=41, N_{AF} = 21).

Table 4. Characterisation of postoperative outcome from TQ analysis. Values are Median(IQR)

AF Substrate	Follow-up	Percentage Recurrence [%]		p value	Percentage Determinism [%]		p value	Entropy of Recurrence [dimensionless]		p value	f-wave Ampl [μV]		p value
Paroxysmal (N=32)	3 month	NSR	AF		NSR	AF		NSR	AF		NSR	AF	
		46.76(15.50)	18.08(28.16)	<0.01	48.02(28.26)	32.19(24.27)	<0.05	4.32(0.63)	3.81(0.63)	<0.05	120(51)	157(153)	p=0.07
	6 month	NSR	AF		NSR	AF		NSR	AF		NSR	AF	
		45.65(19.93)	32.97(35.74)	<0.05	48.25(30.61)	33.77(21.41)	<0.05	4.36(0.65)	3.93(0.40)	<0.005	122(61)	146(107)	N.S.
Persistent (N=30)	3 month	NSR	AF		NSR	AF		NSR	AF		NSR	AF	
		44.27(39.83)	38.00(50.77)	N.S.	51.19(32.26)	43.03(52.07)	N.S.	4.32(0.67)	3.93(1.20)	N.S.	144(46)	154(29)	N.S.
	6 month	NSR	AF		NSR	AF		NSR	AF		NSR	AF	
		46.37(40.07)	37.15(43.62)	N.S.	52.35(31.31)	40.93(39.47)	N.S.	4.36(0.77)	3.77(0.90)	N.S.	142(52)	157(45)	N.S.

AF, atrial fibrillation; NSR, normal sinus rhythm. Paroxysmal AF: N_{NSR}(3-month)=23, N_{AF}(3-month)=9; N_{NSR}(6-month)=20, N_{AF}(6-month)=12; Persistent AF: N_{NSR}(3-month)=20, N_{AF}(3-month)=10; N_{NSR}(6-month)=21, N_{AF}(6-month)=9

Table 5. Characterisation of outcome by continuous AF waveform (PC_3). Values are Median(IQR)

Outcome	Percentage Recurrence [%]		p value	Percentage Determinism [%]		p value	Entropy of Recurrence [dimensionless]		p value
Acute	T-AF	NT-AF		T-AF	NT-AF		T-AF	NT-AF	
	3.02(5.42)	2.36(2.60)	N.S.	10.17(18.39)	7.61(13.49)	N.S.	3.66(0.81)	3.40(0.72)	N.S.
Postoperative (3 months)	NSR	AF		NSR	AF		NSR	AF	
	2.88(5.75)	1.80(1.41)	N.S.	8.30(19.39)	7.61(4.87)	N.S.	3.57(0.91)	3.36(0.45)	N.S.
Postoperative (6 months)	NSR	AF		NSR	AF		NSR	AF	
	2.77(5.79)	2.12(1.29)	N.S.	8.11(18.98)	7.61(5.07)	N.S.	3.56(0.95)	3.41(0.35)	N.S.

T-AF, terminated atrial fibrillation (AF); NT-AF, not terminated AF; NSR, normal sinus rhythm. $N_{T\text{-}AF}$=12, $N_{NT\text{-}AF}$ = 50. At 3-month (6-month) follow-up: N_{NSR}=43, N_{AF} = 19 (N_{NSR}=41, N_{AF} = 21).

Table 6. Prediction of postoperative outcome (NSR vs. AF) at follow-up by TQ analysis

AF Substrate	Follow-up	Predictor	AUC (95% CI)	p value (AUC>0.5)
All (N=62)	3-month	PR [%]	0.63 (0.46, 0.79)	N.S.
		PD [%]	0.64 (0.48, 0.80)	N.S.
		ER	0.67 (0.51, 0.82)	<0.05
	6-month	PR [%]	0.63 (0.48, 0.78)	N.S.
		PD [%]	0.67 (0.53, 0.81)	<0.05
		ER	0.72 (0.58, 0.86)	<0.005
Paroxysmal (N=32)	3-month	PR [%]	0.80 (0.60, 1.00)	<0.01
		PD [%]	0.79 (0.61, 0.97)	<0.05
		ER	0.78 (0.60, 0.96)	<0.05
	6-month	PR [%]	0.71 (0.52, 0.90)	<0.05
		PD [%]	0.75 (0.58, 0.93)	<0.05
		ER	0.81 (0.66, 0.96)	<0.005
Persistent (N=30)	3-month	PR [%]	0.53 (0.31, 0.75)	N.S.
		PD [%]	0.50 (0.27, 0.73)	N.S.
		ER	0.55 (0.30, 0.79)	N.S.
	6-month	PR [%]	0.54 (0.32, 0.76)	N.S.
		PD [%]	0.56 (0.33, 0.79)	N.S.
		ER	0.61 (0.37, 0.85)	N.S.

AUC, area under the curve; PR, percentage recurrence; PD, percentage determinism; ER, entropy of recurrence.

Table 7. Risk of AF relapse(*) by TQ analysis

Predictor	Threshold(†) percentile (value)	HR (95% CI)	p value
PR [%]	25th (18.08)	0.52 (0.28, 0.98)	<0.05
	50th (42.19)	0.48 (0.25, 0.93)	<0.05
	75th (55.52)	0.67 (0.29, 1.50)	N.S.
PD [%]	25th (29.62)	0.52 (0.28, 0.98)	<0.05
	50th (43.54)	0.43 (0.22, 0.85)	<0.05
	75th (61.58)	0.67 (0.29, 1.50)	N.S.
ER [dimensionless]	25th (3.81)	0.35 (0.19, 0.65)	<0.001
	50th (4.19)	0.48 (0.25, 0.93)	<0.05
	75th (4.51)	0.45 (0.18, 1.14)	N.S.

(*) Cox proportional hazard regression model with time to event calculated as follow-up period (3 and 6 month).

(†) Calculated from the preoperative data distribution of the entire population (N=62).

HR, hazard ratio; CI, confidence interval; PR, percentage recurrence; PD, percentage determinism; ER, entropy of recurrence.

Figure 1

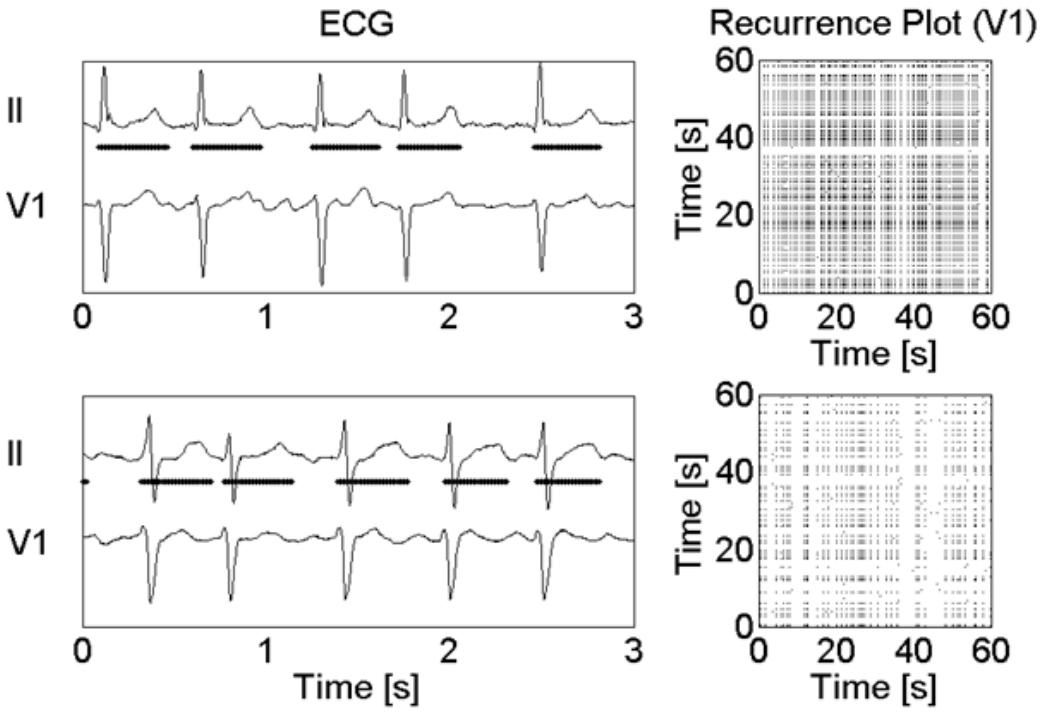

Figure 1. Preprocedural ECG recordings: lead II, V_1 (left panels) and Recurrence Plot of V1 for a patient in sinus rhythm at 6-month follow-up (top panels) and a patient with AF relapse at follow-up (bottom panels). QRS-T intervals are automatically detected from lead II (solid horizontal lines in left panels). In TQ analysis, points corresponding to QRS-T intervals in recurrence matrix are forced to zero (eq. (2) in Appendix). The patient in NSR at follow-up has higher PR (67% vs. 44%), PD (78% vs. 35%), ER (4.93 vs. 3.98) than the patient in AF.

Figure 2

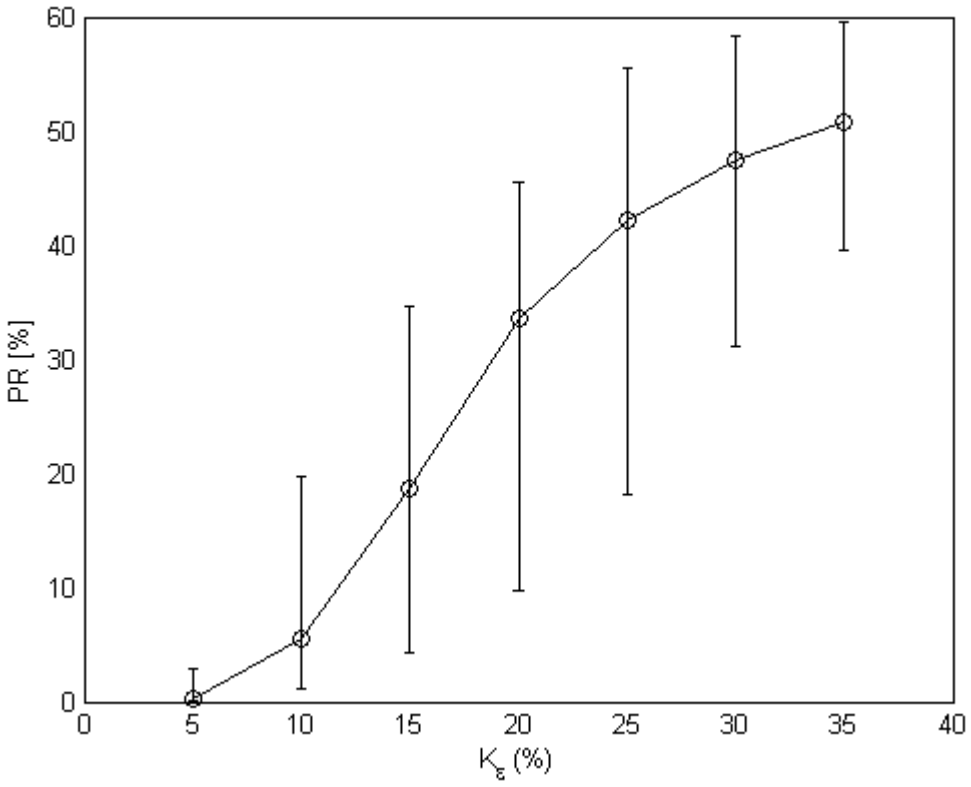

Figure 2. Percentage recurrence distribution in the overall sample (N=62) as a function of threshold factor K_ε for recurrence plot of TQ intervals. Vertical bars indicate inter-quartile range for PR distribution at chosen value of K_ε. Empty circles indicate median value.

Figure 3

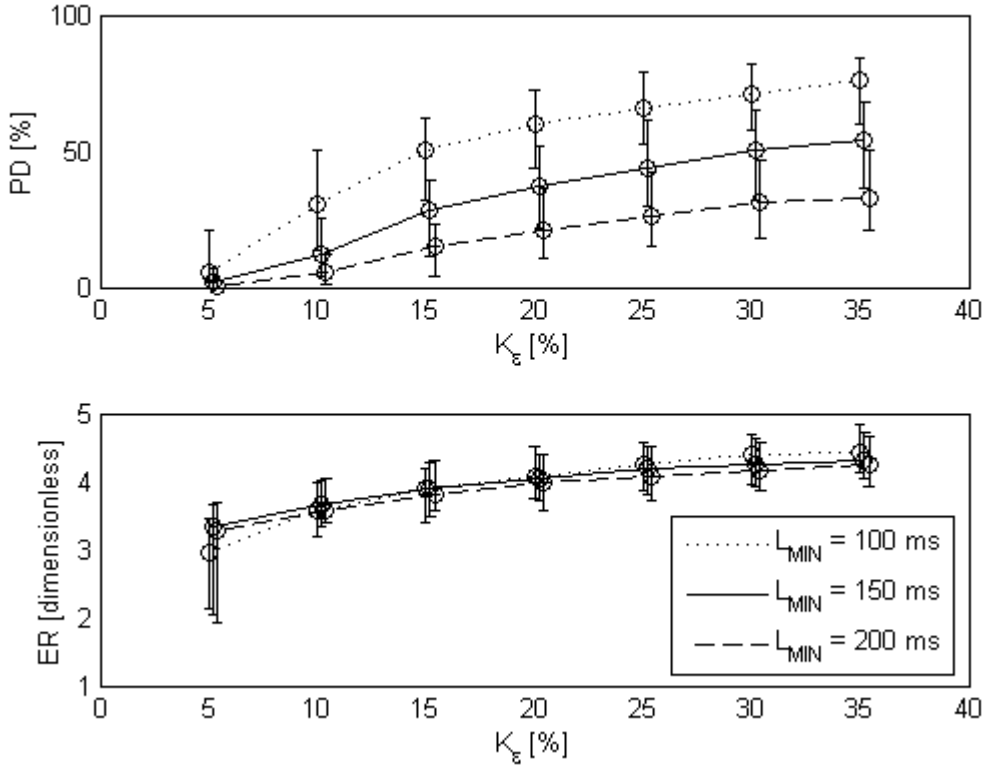

Figure 3. Percentage determinism (top) and entropy of recurrence (bottom) distribution in the overall sample (N=62) as a function of threshold factor K_ε for recurrence plot of TQ intervals, for different values of L_{MIN}. Vertical bars indicate inter-quartile range for index distribution at chosen value of K_ε, empty circle indicates median value.